Veterinary Microbiology 293 (2024) 110101

Contents lists available at ScienceDirect

Veterinary Microbiology

journal homepage: www.elsevier.com/locate/vetmic

Evidence for cross-species transmission of human coronavirus OC43 through bioinformatics and modeling infections in porcine intestinal organoids

Guige Xu [a,b,1], Zhiwen Qiao [c,1], Rick Schraauwen [d], Amine Avan [b], Maikel P. Peppelenbosch [b], Marcel J.C. Bijvelds [b], Shijin Jiang [a,*], Pengfei Li [b,*]

[a] Department of Preventive Veterinary Medicine, College of Veterinary Medicine, Shandong Agricultural University, Taian, Shandong 271018, China
[b] Department of Gastroenterology and Hepatology, Erasmus MC-University Medical Center, Rotterdam, the Netherlands
[c] State Key Laboratory of Crop Biology, College of Horticulture Science and Engineering, Shandong Agricultural University, Taian 271018, China
[d] Department of Pathology, Erasmus MC-University Medical Center, Rotterdam, the Netherlands

ARTICLE INFO

Keywords:
Human coronavirus OC43
PHEV
Evolutionary origin
Cross-species transmission
Porcine intestinal organoids

ABSTRACT

Cross-species transmission of coronaviruses has been continuously posing a major challenge to public health. Pigs, as the major animal reservoirs for many zoonotic viruses, frequently mediate viral transmission to humans. This study comprehensively mapped the relationship between human and porcine coronaviruses through in-depth bioinformatics analysis. We found that human coronavirus OC43 and porcine coronavirus PHEV share a close phylogenetic relationship, evidenced by high genomic homology, similar codon usage patterns and comparable tertiary structure in spike proteins. Inoculation of infectious OC43 viruses in organoids derived from porcine small and large intestine demonstrated that porcine intestinal organoids (pIOs) are highly susceptible to human coronavirus OC43 infection and support infectious virus production. Using transmission electron microscopy, we visualized OC43 viral particles in both intracellular and extracellular compartments, and observed abnormalities of multiple organelles in infected organoid cells. Robust OC43 infections in pIOs result in a significant reduction of organoids viability and widespread cell death. This study bears essential implications for better understanding the evolutionary origin of human coronavirus OC43, and provides a proof-of-concept for using pIOs as a model to investigate cross-species transmission of human coronavirus.

1. Introduction

Coronaviruses comprise a large group of RNA viruses that circulate among human and animals. Seven coronavirus species are known to naturally infect humans, including three highly pathogenic members (SARS-CoV-1, SARS-CoV-2 and MERS-CoV), and four seasonal human coronaviruses (OC43, 229E, NL63, and HKU1) (Li et al., 2020a). Notably, all of these human coronaviruses are thought to have originated from animals, highlighting their zoonotic characteristics (Ma et al., 2020). Among animals known for zoonotic reservoirs, pigs play a pivotal role in harboring and transmitting a range of zoonotic viruses. For example, hepatitis E virus (Ji et al., 2021; Li et al., 2022a) and influenza virus H1N1 (Cheung et al., 2023) are well-recognized to be originated from pigs, but eventually result in millions of infection episodes in humans. In regarding to coronaviruses, several porcine-tropic coronaviruses circulate among farmed and wild pigs, predominantly affecting the pig intestinal system and leading to diarrhea (Liu & Wang, 2021). Importantly, a serological survey to farmed pigs in Japan reported a high prevalence of 91% seropositivity against seasonal human coronavirus OC43 (Hirano et al., 1999). This has raised concerns about the potential cross-species transmission of coronavirus OC43. Although rodents and cattle have been evidenced as two intermediate hosts for coronavirus OC43 (Forni et al., 2017), whether pigs serve as another reservoir necessitates further investigations.

Classically, immortalized cell lines have been widely used for modelling viral diseases. However, these 2D cultured cell lines harbor enormous genetic and epigenetic alterations, which compromise the authenticity in recapitulating virus-host interactions. In recent years,

* Corresponding authors.
E-mail addresses: sjjiang@sdau.edu.cn (S. Jiang), p.li@erasmusmc.nl (P. Li).
[1] These authors contributed equally.

https://doi.org/10.1016/j.vetmic.2024.110101
Received 17 January 2024; Received in revised form 14 April 2024; Accepted 25 April 2024
Available online 26 April 2024

3D-cultured primary organoids derived from tissue-resident stem cells, have emerged as an innovative platform for studying viral pathogenesis and developing antiviral therapies. Organoids are "mini-organs" that more closely mimic the composition, diversity and functionality of cell types of the original tissue. Human-derived organoids have been exquisitely explored for modelling a range of viral infections (Li et al., 2022b; Li et al., 2023). Likewise, the veterinary field has embraced organoid technology, in particular for investigating animal viruses. Porcine intestinal organoids (pIOs) generated from crypt stem cells of porcine small or large intestinal tissues, have been utilized for studying various porcine coronaviruses (Li et al., 2019; Li et al., 2020b; Yang et al., 2022). This pioneering work has collectively demonstrated the advantages of pIOs for recapitulating porcine enteric viral infections.

In this study, we aim to systematically map the evolutionary relationship between human and porcine coronaviruses though multidimensional bioinformatics analysis. Furthermore, we employ pIOs for evaluating the susceptibility and pathogenicity of human coronavirus OC43 to pigs.

2. Materials and methods

2.1. Phylogenetic analysis

Complete viral genomes of seven human and six porcine coronaviruses were retrieved from GeneBank. The included human coronaviruses are SARS-CoV-1, SARS-CoV-2, MERS-CoV, OC43, 229E, HKU1, and NL63. The included porcine coronaviruses are porcine hemagglutinating encephalomyelitis virus (PHEV), transmissible gastroenteritis coronavirus (TGEV), porcine respiratory coronavirus (PRCV), swine acute diarrhea syndrome coronavirus (SADS-CoV), porcine deltacoronavirus (Pd-CoV), and porcine epidemic diarrhea virus (PEDV). Primary alignment of these viral genomes was performed using the MAFFT tool (Yamada et al., 2016), and phylogenetic maximum-likelihood (ML) trees were constructed employing Maga (Tamura et al., 2021). The generated phylogenetic tree was further modified by iTOL (Qiao et al., 2022).

2.2. Codon usage analysis

Representative genomes from each coronavirus species were randomly selected for codon usage analysis by Codon Usage Calculator (Mortazavi et al., 2016). Relative Synonymous Codon Usage (RSCU) values were analyzed to indicate codon usage patterns (Yu et al., 2023). A high RSCU value (RSCU $>$ 1) indicates positive codon bias and is considered a preferred codon, whereas a low RSCU value (RSCU $<$ 1) represents the negative codon bias termed as under-preferred codons. The detailed information on the coronavirus used for analysis is illustrated in Figure S1A and B.

2.3. Protein homology modeling analysis

The spike protein sequences of human coronavirus OC43 (GenBank: AAT84354) and porcine coronavirus PHEV (GenBank: AAY68297) were submitted to Phyre2, with c6nzkB as reference model for homology modeling (Qiao et al., 2022). PyMOL software (version 2.3.3) was used for structure visualization.

2.4. Viruses and cell lines

Vero-E6 and Huh7 cell lines were cultured in Dulbecco's modified Eagle's medium (DMEM, Lonza, Belgium) supplemented with 10% fetal calf serum (FCS, Hyclone, Logan, USA), penicillin (100 IU/mL) and streptomycin (100 mg/mL). LLC-MK2 cells were cultivated in minimal essential medium with Earle's salt (MEM; Gibco, Grand Island, USA) supplemented with 10% (vol/vol) FCS, 1x nonessential amino acids (Sciencell, San Diego, California, USA), 200 mM L-Glutamine (Lonza, Verviers, Belgium), penicillin (100 IU/mL) and streptomycin (100 mg/mL). These cell lines were validated by short tandem repeat typing methods performed by the Pathology Department at Erasmus MC, and mycoplasma negative status was confirmed by monthly testing (commercially performed by GATC Biotech, Konstanz, Germany). Human coronavirus NL63 stock was produced by inoculation in LLC-MK2 cells. Human coronavirus OC43 and 229E stocks were produced by inoculation in Huh7 cells.

2.5. Cultivation of porcine intestinal organoids (pIOs)

The isolation of pIOs was performed as previously described (Vonk et al., 2020). The use of pIOs was approved by the Independent Committee on Ethical Use of Experimental Animals, Rotterdam, according to national guidelines and in accordance with the Basel declaration on experimental research on vertebrates (protocol number: AVD1010020173286). PIOs were cultured in organoid expansion medium (OEM), based on advanced DMEM/F12 (Invitrogen), supplemented with 1% penicillin/streptomycin (Life Technologies), 10 mM HEPES, Glutamax, N2, B27 (all from Invitrogen), 1 μM N-acetylcysteine (Sigma) and the following growth factors: 50 ng/L mouse epidermal growth factor (mEGF), 50% Wnt3a-conditioned medium (WCM) and 10% noggin-conditioned medium (NCM), 20% Rspo1-conditioned medium, 10 μM nicotinamide (Sigma), 10 nM gastrin (Sigma), 500 nM A83–01 (Tocris) and 10 μM SB202190 (Sigma). The medium was refreshed every 2 days, and organoids were passaged 1:3 every 5–7 days.

2.6. Infection of human seasonal coronaviruses in pIOs

PIOs were first mechanically disrupted into broken fragments to increase the infection efficacy. These fragmented organoids were then inoculated with 3.5×10^6 PFU of 229E virus, 5×10^4 PFU of NL63, and 4×10^4 PFU of OC43 virus respectively for 2 hours at 33 °C. After incubation, organoids were washed with advanced DMEM/F12 medium three times to remove viral inoculum. Finally, organoids were embedded in Matrigel, and maintained in OEM at 37 °C with 5% CO^2. To analyze the intracellular viral replication and extracellular viral production, organoids and supernatants were separately harvested at 1 hour post-infection (h.p.i) and 3 days post-infection (d.p.i), and quantified by qPCR in viral RNA level. To quantify the infectious viral titers, fragmented pIOs were inoculated with 4×10^5 PFU of OC43 virus, and then organoids and supernatant were collectively harvested and detected by $TCID_{50}$ assay.

2.7. Quantification of viral genome copy numbers

Seasonal human coronavirus 229E, OC43 and NL63 virus genomes that contain qPCR detection regions were used to generate plasmids as previously described (Li et al., 2022b). Primers used for this study were provided in Table S1. These plasmids were used as templates for quantifying the corresponding coronavirus genome copy numbers. A series of dilutions of plasmid from 10^{-1} to 10^{-8} were prepared and then were amplified and quantified by qRT-PCR to generate a standard curve. The standard curve was generated by plotting the log copy number versus the cycle threshold (CT) value. Coronavirus copy numbers were calculated as following equation: Copy number (molecules/mL) = [concentration (ng/μL) $\times6.022\times10^{23}$ (molecules/mol)]/[length of amplicon$\times$660 (g/mol)$\times10^9$ (ng/g)].

2.8. Immunofluorescence assay

PIOs inoculated with coronavirus OC43 were seeded at μ-Slide 8-well plate (Ibidi GmbH, Germany). PIOs were fixed in 4% paraformaldehyde solution for 15 min at 3 d.p.i. The wells containing organoids were then rinsed 3 times with PBS, followed by permeabilizing with PBS containing 0.2% (vol/vol) Triton X-100 for 10 min. Then the slides were twice rinsed with PBS for 5 min, followed by incubation with blocking solution

(5% donkey serum, 1% bovine serum albumin, 0.2% Triton X-100 in PBS) at room temperature for 1 hour. Next, slides were incubated with primary antibody diluted in blocking solution at 4 °C overnight. Primary antibodies used in this study are as follows: anti-EpCAM antibody (1:1000, rabbit mAb; Abcam), anti-dsRNA antibody (1:500, mouse mAb; Scicons J2), anti-OC43 Nucleocapsid antibody (1:500, mouse mAb; Sigma-Aldrich). Slides were washed 3 times for 5 min each in PBS prior to 1 hour incubation with 1:1000 dilutions of the anti-mouse IgG (H+L, Alexa Fluor® 594), the anti-rabbit IgG (H+L, Alexa Fluor® 488). Nuclei were stained with DAPI (4, 6-diamidino-2-phenylindole; Invitrogen).

2.9. $TCID_{50}$ calculation

Viruses from pIOs and culture supernatants were collectively harvested through three-times freezing and thawing. OC43 viral titer were quantified by using a 50% Tissue Culture Infectious Dose ($TCID_{50}$) assay.

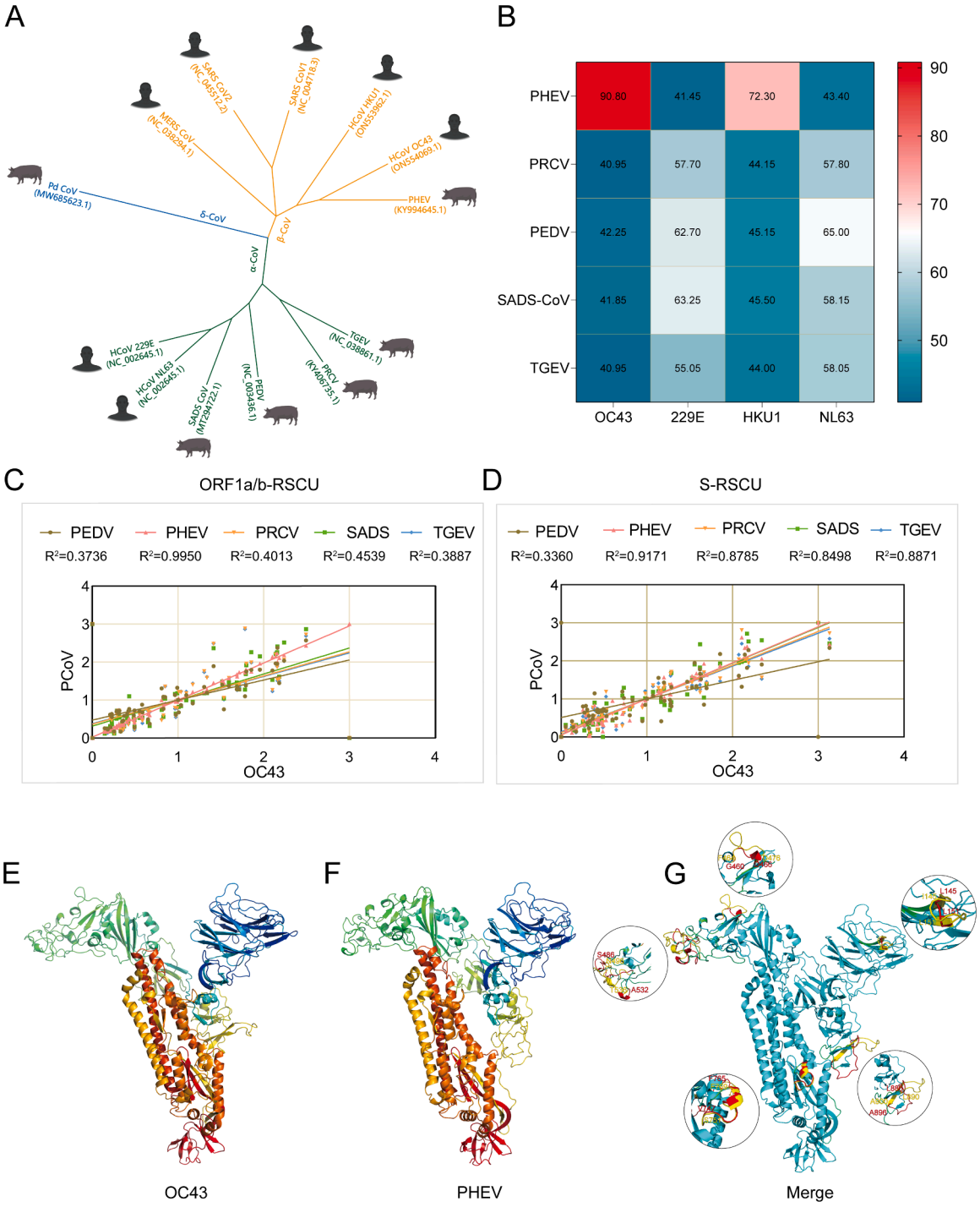

Fig. 1. Multidimensional bioinformatics analysis of human and porcine coronaviruses. (A) Evolutionary analysis of six porcine and seven human coronaviruses. (B) Sequence homology analysis of the complete genomes of nine major coronaviruses affecting humans and pigs. Correlation analysis of RSCU in the ORF1a/b gene (C) and S gene (D) of OC43, PHEV, PEDV, PRCV, SADS CoV, and TGEV. (E) and (F) Tertiary structural models for spike protein of OC43 and PHEV, respectively. (G) The structural matching of spike proteins between OC43 (blue) and PHEV (green). Differences across five structural motifs were magnified and annotated with the starting and ending amino acids (yellow color-OC43; red color-PHEV).

Briefly, ten-fold dilutions of OC43 viruses were inoculated onto Vero-E6 cells that grown in a 96-well plate at approximately 2000 cells/well. The plate was incubated at 33 °C for 7 days, and each well was examined by counting cytopathic effect (CPE). The $TCID_{50}$ value was calculated by using the Reed-Muench method.

2.10. AlamarBlue assay

Culture supernatant of pIOs was discarded and then organoids were incubated with Alamar Blue (Invitrogen, DAL1100, 1:20 dilution in IEM) for 2 h (37 °C). After that, 100 μL medium was collected to assess the metabolic activity of the organoids, with each sample being measured in duplicate. Absorbance was measured using the fluorescence plate reader (CytoFluor Series 4000, Perseptive Biosystems) with excitation at 530/25 nm and emission at 590/35 nm.

2.11. Statistics

Linear correlations of the codon usage and RSCU were estimated by the Pearson coefficients. The statistical significance of differences between means was assessed with the Mann-Whitney test (GraphPad Prism; GraphPad Software Inc., La Jolla, CA). The threshold for statistical significance was defined as $P \leq 0.05$.

3. Results

3.1. Bioinformatics analyses reveal high homology between OC43 and PHEV

To map the evolutionary relationship between human and porcine coronaviruses, we first performed phylogenetic analysis to the known seven human and six porcine coronaviruses. As shown by the phylogenetic tree, except Pd-CoV that independently belongs to δ- CoV, the other human and porcine coronaviruses all fall into the α- and β- CoV groups (Fig. 1A). Interestingly, seasonal human coronaviruses (OC43, HKU1, 229E, NL63) appear to be closely related to porcine coronaviruses from phylogenetic distance. To solidify this finding, we included additional viral strains from NCBI to re-build phylogenetic tree. Remarkably, this analysis identified the closest phylogenetic link between human coronavirus OC43 and PHEV (Figure S1C). This close relationship was consistent with the result from homology analysis, showing a 90.8% genetic similarity between OC43 and PHEV, whereas a comparatively lower homology between other human and porcine coronaviruses (44%-72.3%) (Fig. 1B).

Microorganisms can significantly differ in their codon usage preferences, and codon context constitutes an important step for invading and adapting host speciesism (Arella et al., 2021). Thus, we next compared the relative synonymous codon usage (RSCU) between OC43 and other coronaviruses. Because ORF1a/b and the spike (S) genes constitute over 90% of the coronavirus genome (V'Kovski et al., 2021), our following analysis focused on these two genes. In line with the high genomic similarity between OC43 and PHEV, we found the highest correlation coefficient of RSCU for ORF1a/b gene (R^2=0.9950) and S gene (R^2=0.9171) between OC43 and PHEV (Fig. 1C and D).

Since the spike protein plays a major role in determining viral evolution and host range (Thakor et al., 2022), we then specifically generated the three-dimensional structure of spike protein for OC43 and PHEV (Fig. 1E and F). Notably, the structural analysis showed that the major structures of two spike proteins are overlapped, along with slight disparities in five structural motifs (Fig. 1G). Collectively, these results demonstrated the high homology between seasonal human coronavirus OC43 and porcine coronavirus PHEV, which suggests that pigs may be susceptible to OC43 infection.

3.2. OC43 virus robustly infects porcine intestinal organoids

Next, we utilized 3D cultured organoids derived from porcine small and large intestinal tissues to experimentally investigate the susceptibility to OC43 infection. In parallel, we also inoculated human coronavirus 229E and NL63 in these organoids. Viral genomic RNA was quantified by qRT-PCR and calculated as copy numbers (Figure S3 A-C). As compared between 1 h.p.i and 72 h.p.i, rapid growth of OC43 was evidenced by dramatic increase of viral RNA from 2.0×10^5 to 1.8×10^6 copies/μg RNA from small intestinal organoids, and 1.2×10^5 to 6.0×10^5 copies/μg RNA from large intestinal organoids (Fig. 2A). In contrast, decreased 229E viral RNA copies and no increase of NL63 viral RNA copies were observed at 72 h.p.i (Fig. 2B and C). Robust OC43 virus infection was further demonstrated by immunostaining OC43 Nucleocapsid (N) protein and the viral replicating double-stranded RNA (dsRNA) in both small and large intestinal organoids at 72 h.p.i (Fig. 2D and E).

Next, we profiled the virus propagation kinetics from 1 h.p.i to 7 d.p.i. We first quantified the intracellular viral RNA levels in organoids, and observed a robust growth to approximately 1.53×10^6 copies/μg in both small and large intestinal organoids at 1 d.p.i. Subsequently, the virus slightly decreased to 4.37×10^5 copies/μg in large intestinal organoids, but stably maintained in small intestinal organoids to 7 d.p.i (Fig. 2F). Since the full-life-cycle of virus infection includes intracellular replication and extracellular production, we then quantified the release of viruses into supernatant by qRT-PCR. The amount of released viruses continuously increased from 1 h.p.i up to 7 d.p.i. It finally reached 8.54×10^5 copies/mL supernatant in the small intestinal organoids, and 1.37×10^5 copies/mL supernatant in the large intestinal organoids (Fig. 2G).

To test the infectivity of released extracellular viruses, we inoculated Vero-E6 cell line with culture supernatants derived from OC43-infected pIOs. We found that these released OC43 viruses are highly infectious, as evidenced by clear cytopathic effect (CPE) in Vero-E6 cells (Fig. 2H). The infectious titers of intracellular viruses and released viruses were further quantified by $TCID_{50}$ assay. Compared to undetectable titers (determined as 0 $TCID_{50}$) at 1 h.p.i, approximately $10^{3.17}$ $TCID_{50}$/mL in small intestinal organoids and $10^{2.28}$ $TCID_{50}$/mL in large intestinal organoids were observed at 3 d.p.i (Fig. 2I). Similarly, extracellular infectious viral titers from supernatants peaked at 3 d.p.i, with nearly $10^{1.75}$ $TCID_{50}$/mL in both types of organoids (Fig. 2J).

3.3. Ultrastructural analysis of OC43 infection in porcine intestinal organoids

Transmission electron microscopy (TEM) was used to visualize the infected pIOs samples at 72 h.p.i. Similar to pandemic SARS-CoV-2 virus that replicates and assembles in the cytoplasm (V'Kovski et al., 2021), we observed abundant OC43 viral particles in the cytoplasm of organoid cells (Fig. 3). These virions were measured approximately 80–100 nanometers in diameter exhibiting typical coronavirus morphology. Specifically, massive virions were located in the cytoplasmic vesicles, named large virion-containing vacuole (LVCV) (Fig. 3A, B). We observed virions in both intra- and extracellular compartments of the infected organoid cells (Fig. 3C-F). Notably, we further captured the budding of progeny coronavirus particles (Fig. 3F).

In addition to viral particles, OC43 infection induced abnormalities and disintegration of multiple organelles in organoid cells. For instance, mitochondria clustering around LVCV, appeared swelling and progressive cristae disappearance (Fig. 3A, B). Apoptotic bodies, a key marker of apoptosis and programmed cell death, were visualized in organoid cells (Fig. 3E). Intriguingly, we observed multiple vesicle packets surrounding the LVCV (Fig. 3D), which has been previously described in SARS-CoV infected cells (Knoops et al., 2008). In severely infected organoid cells, we found a range of advanced cell degradation, including extensive cytoplasmic vacuolization and depletion of organelles (Fig. 3G),

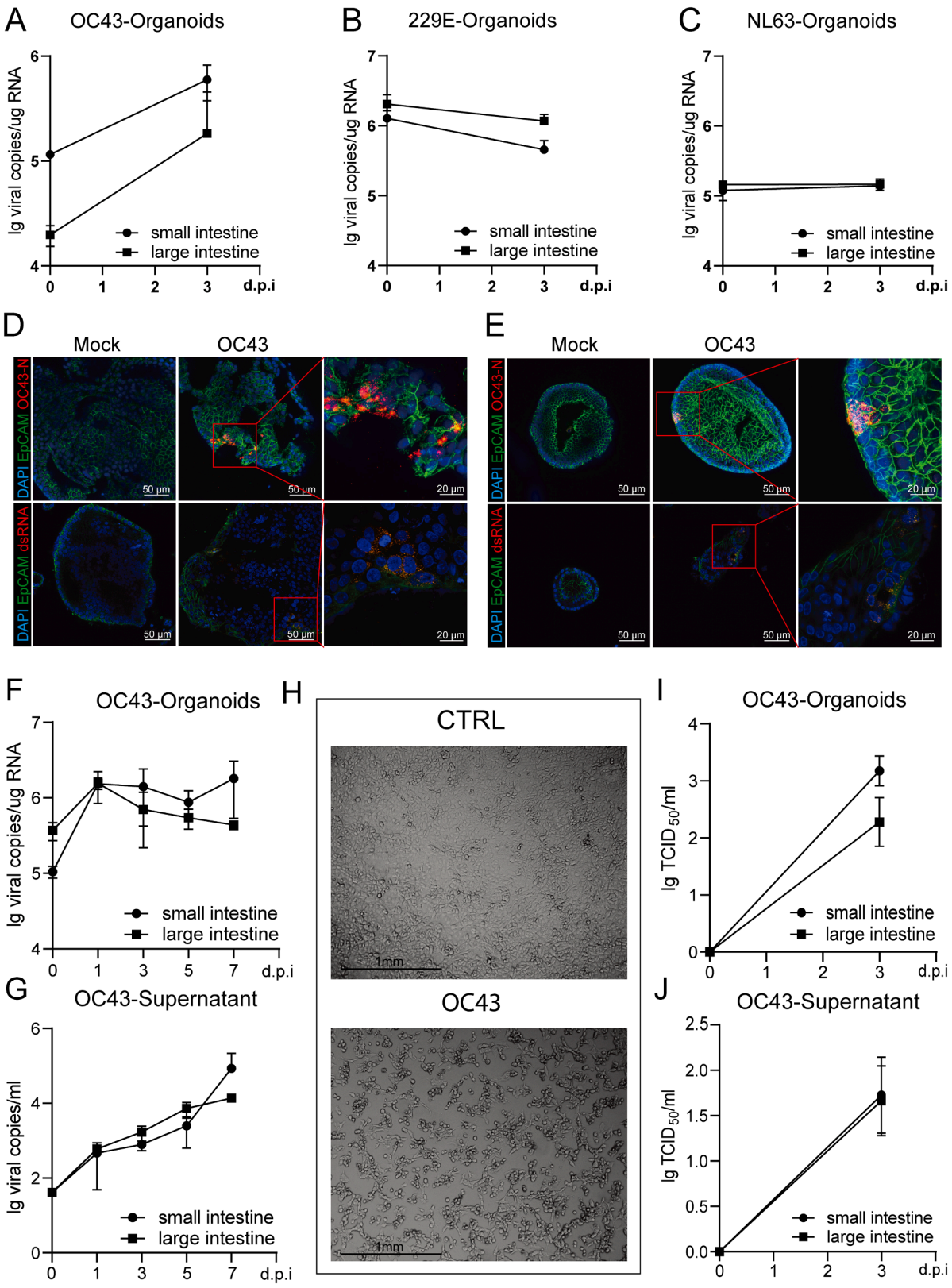

Fig. 2. Characterizing the susceptibility of pIOs to human seasonal coronaviruses. Dynamics of intracellular viral RNA copies of OC43 (A), 229E (B), and NL63 (C) in pIOs from 1 h.p.i to 72 h.p.i (n= 3). Immunofluorescence staining for viral replicating double-stranded RNA (dsRNA) and OC43 N protein in OC43 infected porcine small (D) and large (E) intestinal organoids. Dynamics of intracellular (F) and extracellular (G) OC43 viral RNA copies in pIOs from 1 h.p.i to 7 d.p.i (n= 3). (H) Optical visualization of Vero-E6 cells after 5 days infection by OC43 viruses derived from supernatant of infected pIOs. The infectious titer of intracellular (**I**) and extracellular (**J**) OC43 viruses from 1 h.p.i to 72 h.p.i (n= 4). In (A)-(C), (F), (G), (I) and (J), number '0' in the X axis represents 1 h.p.i.

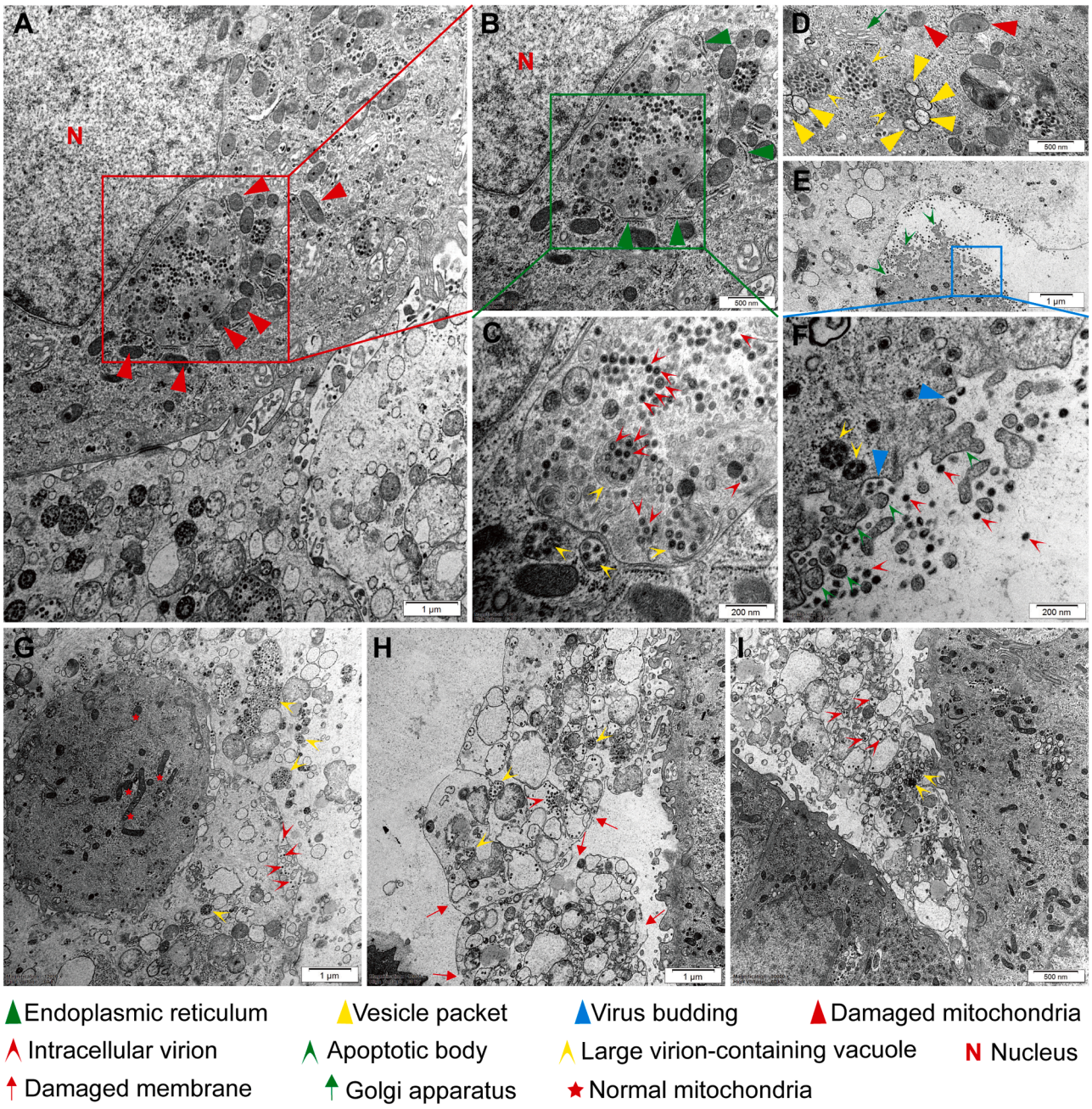

Fig. 3. Transmission electron microscopy (TEM) analysis for coronavirus OC43 infected pIOs. (A) and (B) Representative TEM visualized large circular organelles containing numerous virions (red frame, scale bar= 1 μm; green frame, scale bar= 500 nm). Red arrows indicated mitochondria with abnormal morphology. (C) Magnification view for virions in large circular organelles. (D) Representative TEM visualized multiple vesicle packets surrounding the large virion-containing vacuole. (E) and (F) TEM visualized the process of virus budding and formation of apoptotic bodies. Cellular damages including organelles depletion (G), cellular membrane disintegration (H) and membrane disappearance (I) were observed by TEM.

cellular membrane disintegration (Fig. 3H), and even membrane disappearance (Fig. 3I).

3.4. OC43 infection causes pathogenic effects in organoids

Our previous work has demonstrated that OC43 infection can induce severe cytopathogenesis in human lung organoids (Li et al., 2022b). In this study, we found extensive pathogenic alterations in OC43 infected pIOs visualized by TEM. We further measured cell viability by alamarblue assay at 1.d.p.i and 5 d.p.i. In both porcine small and large intestinal organoids, significantly reduced cell viability ($p<0.05$) was observed at 5 d.p.i (Fig. 4A and B). Morphological analysis during the infection period revealed evident abnormalities and disintegration in OC43-infected organoids (Figure S4). Propidium iodide (PI) and Hoechst staining identified widespread of dying cells with fragmented nuclei within the infected organoids (Fig. 4C and D). These results collectively demonstrated that OC43 virus can induce severe cytopathogenic effects in pIOs.

4. Discussion

Coronaviruses have been continuously emerging and causing countless infection episodes among human and animals (Miranda et al., 2021). The fact that many coronaviruses are capable of cross-species

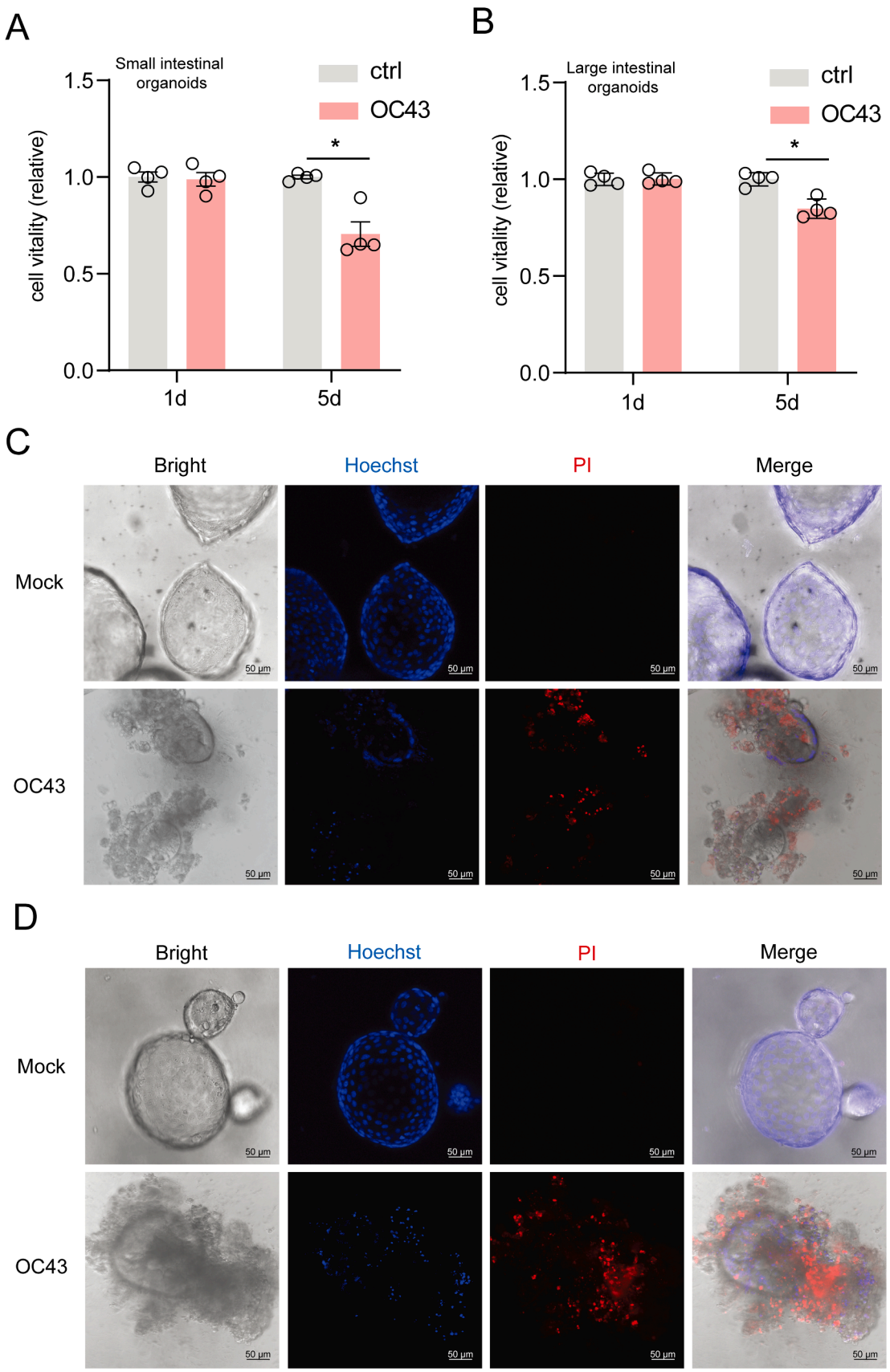

Fig. 4. Evaluation of cytopathogenesis induced by OC43 infection in pIOs. (A) and (B) Cell viability of porcine small and large intestinal organoids at 1 d.p.i and 5 d.p.i (n= 4). Fluorescence staining of dead cells (PI; red color), cell nucleus (DAPI; blue color) and bright field at 5 d.p.i in porcine small (C) and large (D) intestinal organoids. *$P < 0.05$.

transmission has made it a major risk to public health. In this study, we performed a multidimensional analysis among human and porcine coronaviruses to compare their phylogenetic relationship, genome-wide and protein structural homology, and codon usage patterns. Our results determined a close evolutionary relationship and genomic homology between human coronavirus OC43 and porcine coronavirus PHEV, which indicates a shared evolutionary origin of the two viruses. This finding is in line with the previous speculation regarding a common ancestry between OC43 and PHEV (Vijgen et al., 2006). In addition, we demonstrated the similar codon usage patterns and comparable tertiary structures of spike proteins among OC43 and PHEV, which suggested a similar host tropism of these two viruses.

Previously, human coronavirus OC43 was thought to be originated from rodents (e.g., mouse), and then transmitted to cattle as an intermediate reservoir before leaping to humans (Vijgen et al., 2005; Xie et al., 2022). However, our analysis suggests that OC43 and PHEV may share a similar host tropism, with pigs potentially serving as the natural host. This notion was further supported by our investigation into codon usage patterns, as the codon usage of OC43 exhibited a closer resemblance to that of pigs in comparison to cattle and mouse, albeit slightly less than that of human (Figure S2). This adaption in codon usage represented the potential preference of coronavirus OC43 to pigs over other animals. Intriguingly, despite their close relationship in evolutionary and genetic homology, OC43 and PHEV exhibit distinct patterns of seasonality. OC43 predominantly circulates during the winter months, whereas PHEV appears to have no seasonality (Li et al., 2022b; Mora-Díaz et al., 2019). We postulate that it is because the majority of PHEV infections occur in domestic pigs, which are typically raised in temperature-controlled livestock farms.

Since the advent of human intestinal organoids in 2009 (Sato et al., 2009), adult stem cell-derived organoids have been extensively isolated and cultured from a variety of human organs/tissues (Barker et al., 2010; Snippert et al., 2010). Learning from human organoid technology, researchers have successfully developed intestinal organoids from farm animals for studying animal nutrition and microbial infection (Beaumont et al., 2021). Specifically, porcine intestinal organoids featuring villi and crypt-like domains, are self-renewal and capable of growing into three-dimensional structures (Ma et al., 2022). Compared to classical porcine enteric cell lines, these intestinal organoids can more closely emulate *in vivo* gut environments, provide authentic host receptors and display more sophisticated responses towards microbial invasions (Li et al., 2022b; Li et al., 2022c). In the present study, we extended the application of porcine organoids to investigate potential cross-species transmission of human coronavirus OC43. Through multiple virological assays, we demonstrated that porcine small and large intestinal organoids are permissive to human coronavirus OC43 replication and infectious virus production. Notably, we captured virions in both intracellular and extracellular compartments in organoid cells by TEM visualization. These observations suggested that pIOs support the full life cycle of human coronavirus OC43. In contrast to the robust infectivity of OC43 in pIOs, the other two seasonal human coronaviruses — NL63 and 229E failed to replicate in these organoids. This disparity underscored the capability of pIOs to reflect the authentic infectivity of different viruses.

Human coronavirus OC43, primarily a respiratory virus leading to upper respiratory infections. However, it can also cause intestinal manifestations such as diarrhoea in many patients (Vabret et al., 2008). In this study, we observed that OC43 infection in pIOs can dramatically alter organoid morphology, resulting in disintegration and fragmentation of infected organoid cells. These pathological effects indicate that OC43 infection is capable of injuring the epithelial barrier of porcine intestines. If such infection and pathogenicity are confirmed in pigs, veterinarians shall be cautious of gastrointestinal illness in pigs due to OC43 infection, and further prevention or treatment strategies should be considered. More concerning is the possibility of co-existence of porcine coronavirus and human coronavirus OC43 in pigs, which may accelerate the emergence of recombinant variants. These recombinant variants might pose a spillover risk to humans, especially considering our frequent contact with pigs and pork products in daily life. Thus, we call for future research to investigate the prevalence of OC43 virus in domestic pigs, wild boars and related pork products.

In summary, we have systematically mapped the evolutionary relationship between human and porcine coronaviruses, and clarified the high similarity between human coronavirus OC43 and porcine coronavirus PHEV at a multidimensional level. Moreover, we have demonstrated that porcine intestinal organoids support the full life cycle of human coronavirus OC43. These findings shall help to better understand the host range of OC43, and its potential of cross-species transmission from pig to human.

CRediT authorship contribution statement

Guige Xu: Writing – original draft, Project administration, Methodology, Investigation, Formal analysis. **Zhiwen Qiao:** Methodology, Formal analysis, Data curation. **Rick Schraauwen:** Visualization, Investigation. **Amine Avan:** Formal analysis. **Maikel P. Peppelenbosch:** Writing – review & editing. **Marcel J. C. Bijvelds:** Resources, Methodology. **Shijin Jiang:** Supervision, Conceptualization. **Pengfei Li:** Writing – review & editing, Writing – original draft, Supervision, Conceptualization.

Declaration of Competing Interest

The authors declare that they have no conflicts of interest with the contents of this article.

Acknowledgements

This work was supported by a pandemic preparedness grant (grant number 10710032310013) from the Care Research Netherlands (ZonMw) to P.L., and the China Scholarship Council for funding PhD fellowship to G.X. (no. 202208370136).

Appendix A. Supporting information

Supplementary data associated with this article can be found in the online version at doi:10.1016/j.vetmic.2024.110101.

References

Arella, D., Dilucca, M., Giansanti, A., 2021. Codon usage bias and environmental adaptation in microbial organisms. Mol. Genet Genom. 296, 751–762.
Barker, N., Huch, M., Kujala, P., van de Wetering, M., Snippert, H.J., van Es, J.H., Clevers, H., 2010. Lgr5(+ve) stem cells drive self-renewal in the stomach and build long-lived gastric units in vitro. Cell Stem Cell 6, 25–36.
Beaumont, M., Blanc, F., Cherbuy, C., Egidy, G., Giuffra, E., Lacroix-Lamande, S., Wiedemann, A., 2021. Intestinal organoids in farm animals. Vet. Res 52, 33.
Cheung, J., Bui, A.N., Younas, S., Edwards, K.M., Nguyen, H.Q., Pham, N.T., Dhanasekaran, V., 2023. Long-Term Epidemiology and Evolution of Swine Influenza Viruses, Vietnam. Emerg. Infect. Dis. 29, 1397–1406.
Forni, D., Cagliani, R., Clerici, M., Sironi, M., 2017. Molecular Evolution of Human Coronavirus Genomes. Trends Microbiol 25, 35–48.
Hirano, N., Suzuki, Y., Haga, S., 1999. Pigs with highly prevalent antibodies to human coronavirus and swine haemagglutinating encephalomyelitis virus in the Tohoku District of Japan. Epidemiol. Infect. 122, 545–551.
Ji, Y., Li, P., Jia, Y., Wang, X., Zheng, Q., Peppelenbosch, M.P., Pan, Q., 2021. Estimating the burden and modeling mitigation strategies of pork-related hepatitis E virus foodborne transmission in representative European countries. One Health 13, 100350.
Knoops, K., Kikkert, M., Worm, S.H., Zevenhoven-Dobbe, J.C., van der Meer, Y., Koster, A.J., Snijder, E.J., 2008. SARS-coronavirus replication is supported by a reticulovesicular network of modified endoplasmic reticulum. PLoS Biol. 6, e226.
Liu, Q., Wang, H.Y., 2021. Porcine enteric coronaviruses: an updated overview of the pathogenesis, prevalence, and diagnosis. Vet. Res Commun. 45, 75–86.
Li, L., Fu, F., Guo, S., Wang, H., He, X., Xue, M., Liu, P., 2019. Porcine Intestinal Enteroids: a New Model for Studying Enteric Coronavirus Porcine Epidemic Diarrhea Virus Infection and the Host Innate Response. J. Virol. 93, e01682–18.

Li, P., Ji, Y., Li, Y., Ma, Z., Pan, Q., 2022a. Estimating the global prevalence of hepatitis E virus in swine and pork products. One Health 14, 100362.
Li, P., Liu, J., Ma, Z., Bramer, W.M., Peppelenbosch, M.P., Pan, Q., 2020a. Estimating Global Epidemiology of Low-Pathogenic Human Coronaviruses in Relation to the COVID-19 Context. J. Infect. Dis. 222, 695–696.
Li, P., Li, Y.L., Wang, Y.J., Liu, J.Y., Lavrijsen, M., Li, Y., Pan, Q.W., 2022c. Recapitulating hepatitis E virus-host interactions and facilitating antiviral drug discovery in human liver-derived organoids. Sci. Adv. 8, eabj5908.
Li, P., Pachis, S.T., Xu, G., Schraauwen, R., Incitti, R., de Vries, A.C., Pan, Q., 2023. Mpox virus infection and drug treatment modelled in human skin organoids. Nat. Microbiol 8, 2067–2079.
Li, P., Wang, Y., Lamers, M.M., Lavrijsen, M., Iriondo, C., de Vries, A.C., Pan, Q., 2022b. Recapitulating infection, thermal sensitivity and antiviral treatment of seasonal coronaviruses in human airway organoids. EBioMedicine 81, 104132.
Li, Y., Yang, N., Chen, J., Huang, X., Zhang, N., Yang, S., Liu, G., 2020b. Next-Generation Porcine Intestinal Organoids: an Apical-Out Organoid Model for Swine Enteric Virus Infection and Immune Response Investigations. J. Virol. 94, e01006–20.
Ma, P., Fang, P., Ren, T., Fang, L., Xiao, S., 2022. Porcine Intestinal Organoids: Overview of the State of the Art. Viruses 14, 1110.
Ma, Z., Li, P., Ikram, A., Pan, Q., 2020. Does Cross-neutralization of SARS-CoV-2 Only Relate to High Pathogenic Coronaviruses? Trends Immunol. 41, 851–853.
Miranda, C., Silva, V., Igrejas, G., Poeta, P., 2021. Genomic evolution of the human and animal coronavirus diseases. Mol. Biol. Rep. 48, 6645–6653.
Mora-Díaz, J.C., Piñeyro, P.E., Houston, E., Zimmerman, J., Giménez-Lirola, L.G., 2019. Porcine Hemagglutinating Encephalomyelitis Virus: A Review. Front Vet. Sci. 6, 53.
Mortazavi, M., Zarenezhad, M., Alavian, S.M., Gholamzadeh, S., Malekpour, A., Ghorbani, M., Fakhrzad, A., 2016. Bioinformatic Analysis of Codon Usage and Phylogenetic Relationships in Different Genotypes of the Hepatitis C Virus. Hepat. Mon. 16, e39196.
Qiao, Z.W., Wang, D.R., Wang, X., You, C.X., Wang, X.F., 2022. Genome-wide identification and stress response analysis of cyclophilin gene family in apple (Malus x domestica). BMC Genom. 23, 806.
Sato, T., Vries, R.G., Snippert, H.J., van de Wetering, M., Barker, N., Stange, D.E., Clevers, H., 2009. Single Lgr5 stem cells build crypt-villus structures in vitro without a mesenchymal niche. Nature 459, 262–265.
Snippert, H.J., Haegebarth, A., Kasper, M., Jaks, V., van Es, J.H., Barker, N., Clevers, H., 2010. Lgr6 marks stem cells in the hair follicle that generate all cell lineages of the skin. Science 327, 1385–1389.
Tamura, K., Stecher, G., Kumar, S., 2021. MEGA11: Molecular Evolutionary Genetics Analysis Version 11. Mol. Biol. Evol. 38, 3022–3027.
Thakor, J.C., Dinesh, M., Manikandan, R., Bindu, S., Sahoo, M., Sahoo, D., Chaicumpa, W., 2022. Swine coronaviruses (SCoVs) and their emerging threats to swine population, inter-species transmission, exploring the susceptibility of pigs for SARS-CoV-2 and zoonotic concerns. Vet. Q. 42, 125–147.
V'Kovski, P., Kratzel, A., Steiner, S., Stalder, H., Thiel, V., 2021. Coronavirus biology and replication: implications for SARS-CoV-2. Nat. Rev. Microbiol 19, 155–170.
Vabret, A., Dina, J., Gouarin, S., Petitjean, J., Tripey, V., Brouard, J., Freymuth, F., 2008. Human (non-severe acute respiratory syndrome) coronavirus infections in hospitalised children in France. J. Paediatr. Child Health 44, 176–181.
Vijgen, L., Keyaerts, E., Lemey, P., Maes, P., Van Reeth, K., Nauwynck, H., Van Ranst, M., 2006. Evolutionary history of the closely related group 2 coronaviruses: porcine hemagglutinating encephalomyelitis virus, bovine coronavirus, and human coronavirus OC43. J. Virol. 80, 7270–7274.
Vijgen, L., Keyaerts, E., Moes, E., Thoelen, I., Wollants, E., Lemey, P., Van Ranst, M., 2005. Complete genomic sequence of human coronavirus OC43: molecular clock analysis suggests a relatively recent zoonotic coronavirus transmission event. J. Virol. 79, 1595–1604.
Vonk, A.M., van Mourik, P., Ramalho, A.S., Silva, I.A.L., Statia, M., Kruisselbrink, E., Beekman, J.M., 2020. Protocol for Application, Standardization and Validation of the Forskolin-Induced Swelling Assay in Cystic Fibrosis Human Colon Organoids. STAR Protoc. 1, 100019.
Xie, P., Fang, Y., Baloch, Z., Yu, H., Zhao, Z., Li, R., Xia, X., 2022. A Mouse-Adapted Model of HCoV-OC43 and Its Usage to the Evaluation of Antiviral Drugs. Front Microbiol 13, 845269.
Yamada, K.D., Tomii, K., Katoh, K., 2016. Application of the MAFFT sequence alignment program to large data-reexamination of the usefulness of chained guide trees. Bioinformatics 32, 3246–3251.
Yang, N., Zhang, Y., Fu, Y., Li, Y., Yang, S., Chen, J., Liu, G., 2022. Transmissible Gastroenteritis Virus Infection Promotes the Self-Renewal of Porcine Intestinal Stem Cells via Wnt/beta-Catenin Pathway. J. Virol. 96, e0096222.
Yu, J., Han, Y., Xu, H., Han, S., Li, X., Niu, Y., Zhang, F., 2023. Structural divergence and phylogenetic relationships of Ajania (Asteraceae) from plastomes and ETS. BMC Genom. 24, 602.